DOI: 10.1002/ejic.201000213

Ureaphosphanes as Hybrid, Anionic or Supramolecular Bidentate Ligands for Asymmetric Hydrogenation Reactions

Jurjen Meeuwissen,[a] Remko Detz,[b] Albertus J. Sandee,[a,c] Bas de Bruin,[a] Maxime A. Siegler,[d] Anthony L. Spek,[d] and Joost N. H. Reek*[a]

Keywords: Asymmetric hydrogenation / Rhodium / Phosphorus ligands / Coordination chemistry / Hydrogen bonds

We report the coordination behavior of ureaphosphane ligand 1-[2-(diphenylphosphanyl)ethyl]-3-phenylurea (**L1**) towards different rhodium precursor complexes. Depending on the nature of the anion and the ligand/metal ratio, **L1** acts either as a hybrid *P,O*-coordinating chelate, as an anionic *P,N*-coordinating chelate or as a supramolecular (hydrogen-bonded) bidentate ligand. The different types of complexes were investigated in the asymmetric hydrogenation of three olefinic substrates using ureaphosphanes **L2** and **L3**, which are chiral analogues of **L1**. For methyl 2-acetamidoacrylate (**S1**) and dimethyl itaconate (**S2**) the neutral complex [Rh(**L2**-κ^2*P,N*)(cod)], containing an anionic *P,N*-coordinating ureaphosphane ligand, provided the best enantioselectivity (69.2 and 24.3%, respectively). For *N*-(3,4-dihydro-2-naphthalenyl)acetamide (**S3**) the best enantioselectivity was obtained with the cationic complex [Rh(**L3**-κ^2*P,O*)(nbd)]BF_4, containing a hybrid *P,O*-coordinating ureaphosphane ligand (86.1%).

Introduction

The use of supramolecular approaches in ligand design for transition metal catalysis is an upcoming research field, which has already brought forth several success stories within a relatively short period of time.[1] The design of the ligand structure and the binding motif are crucial aspects herein. Examples of binding motifs that have been successfully employed for supramolecular architectures are hydrogen bonding,[2] metal–ligand[3] and ionic[4] interactions. In some cases, the binding motif can also show affinity for the metal center or the counterion of the complex, potentially giving rise to unexpected new (supramolecular) coordination geometries. Although these complexes are in first instance unwanted, they can provide important insight in the mechanistic aspects of the binding motif in catalysis and may lead to new useful catalysts.

We[5,6] and the group of Love[8] have recently introduced urea-functionalized ligands, which form a supramolecular hydrogen-bonded bidentate ligand via a self-assembly process in presence of a transition metal. Ureaphosphanes are part of this type of ligands and were used as supramolecular bidentate ligands in the rhodium-catalyzed asymmetric hydrogenation of several (industrially relevant) substrates.[7] In addition, we showed that ureaphosphanes also can be employed as hybrid *P,O*-coordinating bidentate ligands in the asymmetric hydrogenation of cyclic enamides.[9] In this contribution, we report on the different coordination behavior of ureaphosphanes, depending on the conditions applied. The new ureaphosphane-rhodium(I) complexes have been characterized in detail using NMR spectroscopy, mass spectrometry, IR spectroscopy, X-ray crystallography and computational methods. In addition, these new complexes were investigated in the asymmetric hydrogenation reaction to evaluate the effect of the coordination behavior on the enantioselectivity in catalysis.

Results and Discussion

We investigated the coordination behavior of ureaphosphanes towards different rhodium(I) precursors using 1-[2-(diphenylphosphanyl)ethyl]-3-phenylurea (**L1**) as a model compound. The structure of **L1** consists of a diphenyl phosphane backbone, which is connected via a flexible spacer to a phenyl urea moiety. In a dilution study of **L1** in $CDCl_3$, monitored by ^1H NMR spectroscopy, the urea-protons showed a strong shift to low field as a function of concentration, which is indicative of (intermolecular) hydrogen bonding via self-association of the urea moieties.[10,11] Interestingly, this property can be utilized for the formation of

[a] Homogeneous and Supramolecular Catalysis, Van 't Hoff Institute for Molecular Sciences,
Nieuwe Achtergracht 166, 1018 WV Amsterdam, The Netherlands
Fax: +31-20 5255604
E-mail: j.n.h.reek@uva.nl
[b] InCatT B.V.,
Roetersstraat 35, 1018 WB Amsterdam, The Netherlands
[c] BASF Nederland B.V.,
Strijkviertel 67, 3454 PK De Meern, The Netherlands
[d] Crystal and Structural Chemistry, Bijvoet Centre for Biomolecular Research, Faculty of Science, Utrecht University, Padualaan 8, 3584 CH Utrecht, The Netherlands
Supporting information for this article is available on the WWW under http://dx.doi.org/10.1002/ejic.201000213.

a supramolecular bidentate ligand connected via (intramolecular) hydrogen bonding. Addition of two equivalents of **L1** to the cationic rhodium precursor $[Rh(nbd)_2]BF_4$ (nbd = 2,5-norbornadiene) in $CDCl_3$, led to the appearance of a doublet in the $^{31}P\{^1H\}$ NMR spectrum, resonating at δ = 18.4 ppm ($^1J_{P\text{-}Rh}$ = 152 Hz), which corresponds to a bisligated complex (**C1**) in a *cis* geometry (Scheme 1). In the ^1H NMR spectrum, the urea protons in this complex showed a large downfield shift with respect to the free ligand, which is indicative of hydrogen bonding. The DFT-optimized structure of **C1** supports the structure of a supramolecular bidentate ligand that is connected via a bifurcated hydrogen bond (1.925 and 2.057 Å) between the urea moieties (Figure 1).

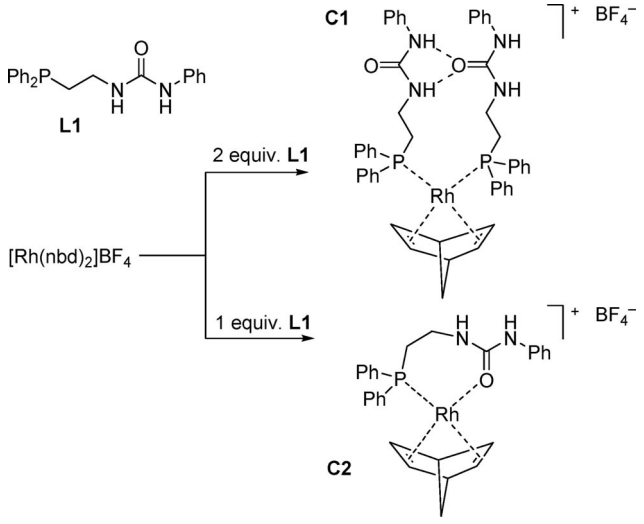

Scheme 1. Reactivity of **L1** with $[Rh(nbd)_2]BF_4$.

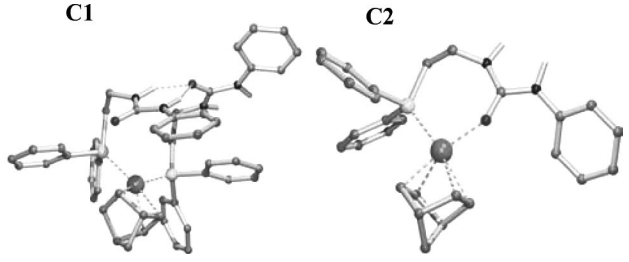

Figure 1. DFT [BP86, SV(P)]-optimized structures of **C1** [Rh(**L1**)$_2$(nbd)]BF_4 and **C2** [Rh(**L1**-κ^2*P,O*)(nbd)]BF_4. CH hydrogen atoms and the BF_4^- counterion have been omitted for clarity.

However, after addition of only one equivalent of **L1** to $[Rh(nbd)_2]BF_4$ a different complex (**C2**) was formed and the ureaphosphane acts as a hybrid *P,O*-coordinating bidentate ligand (Scheme 1).[9] The $^{31}P\{^1H\}$ NMR spectrum showed a doublet, resonating at δ = 31.4 ppm ($^1J_{P\text{-}Rh}$ = 170 Hz). Mass spectrometry and ^1H NMR spectroscopy indicated that the structure of **C2** is of the form [Rh(**L1**-κ^2*P,O*)(nbd)]BF_4, containing only one ligand and one nbd coordinated to the metal center. In the $^{13}C\{^1H\}$ NMR spectrum of **C2** the urea carbonyl signal was shifted downfield with $\delta \approx 5.5$ ppm with respect to the free ligand. This shift revealed that **L1** coordinated to the rhodium in a hybrid (*P,O*-coordinating) bidentate fashion, forming a seven-membered chelate ring.[12,13] The IR spectroscopic data provided support that **L1** formed a hybrid chelate, showing a typical shift of the coordinating urea carbonyl to lower wavenumber (**L1**: 1672 cm^{-1}, **C2**: 1572 cm^{-1}). The DFT-optimized structure of **C2** showed the hybrid coordination mode of **L1** that is consistent with experimental observations (Figure 1).

The coordination behavior of **L1** to the neutral rhodium precursors $[\{RhCl(cod)\}_2]$ (cod = 1,5-cyclooctadiene), $[Rh(acac)(CO)_2]$ (acac = acetylacetonate) and [Rh(acac)(cod)] was subsequently investigated (Scheme 2). Upon addition of one equivalent of **L1** to half an equivalent of $[\{RhCl(cod)\}_2]$ (Rh/**L1** = 1:1) in $CDCl_3$ the $^{31}P\{^1H\}$ NMR spectrum showed a doublet, resonating at δ = 21.1 ppm ($^1J_{P\text{-}Rh}$ = 148 Hz), which indicated that a new complex (**C3**) has been formed.[14] The ^1H NMR spectrum and mass spectrometry revealed that the cod remained coordinated, which means that **C3** is of the form [RhCl(**L1**)(cod)]. Remarkably, the aliphatic urea proton (CH_2NH) of **L1** showed a relatively large downfield shift (ca. 0.9 ppm) with respect to the free ligand, while the shift of the phenylic urea proton (N*H*Ph) was almost unchanged. Therefore, the aliphatic urea proton is likely hydrogen-bonded to the chloride, forming a seven-membered chelate ring.[15] This was supported by a dilution study of **C3** that showed that the shift of the aliphatic proton is practically independent of the concentration in a range of 10–40 mM, which is indicative of an intramolecular hydrogen bond.[10] The DFT-optimized structure of **C3** supports the presence of a hydrogen bond (2.236 Å) between the aliphatic urea proton and the chloride (Figure 2).

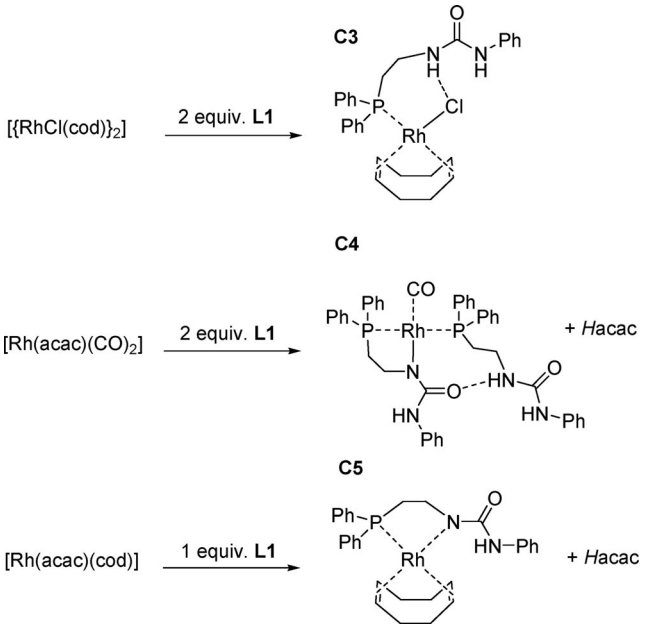

Scheme 2. Reactivity of **L1** with $[\{RhCl(cod)\}_2]$, $[Rh(acac)(CO)_2]$ and [Rh(acac)(cod)].

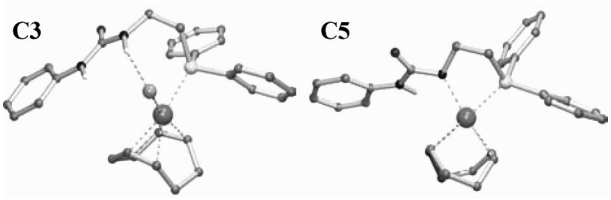

Figure 2. DFT [BP86, SV(P)]-optimized structures of **C3** [RhCl(**L1**)(cod)] and **C5** [Rh(**L1**-κ^2*P*,*N*)(cod)]. CH hydrogen atoms have been omitted for clarity.

When two equivalents of **L1** were added to [Rh(acac)-$(CO)_2$] in $CDCl_3$ the $^{31}P\{^1H\}$ NMR spectrum showed two doublets of doublets, resonating at δ = 19.7 ppm ($^1J_{P\text{-}Rh}$ = 136 Hz) and δ = 52.2 ppm ($^1J_{P\text{-}Rh}$ = 129 Hz), each with a large phosphorus-phosphorus coupling constant ($^2J_{P,P}$ = 310 Hz), indicating that a new complex (**C4**) has been formed that contains two inequivalent phosphorus ligands in a mutual *trans* geometry (Figure 3).[16] Remarkably, the ^1H NMR spectrum showed only one of the aliphatic urea protons and the presence of *H*acac, which is presumably explained by the transfer of the acidic aliphatic urea proton from one of the ligands to the acac$^-$ ligand via an acid–base reaction. This behavior was previously observed for METAMORPhos ligands that contain a very acidic sulfonamide proton and react in a similar manner with [Rh(acac)$(CO)_2$].[2a,17]

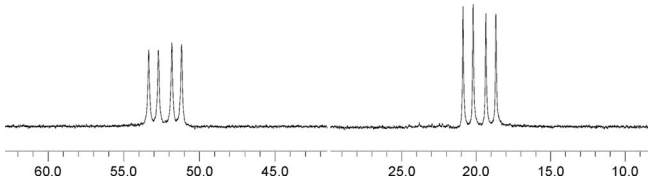

Figure 3. $^{31}P\{^1H\}$ NMR spectrum of **C4** [Rh(**L1**-κ^2*P*,*N*)(**L1**-κ*P*)(CO)].

Single crystals of **C4**, suitable for X-ray analysis, were obtained by slow diffusion of a layer of hexanes on top of a solution of **C4** in CD_2Cl_2. The solid-state structure showed to be consistent with the solution structure, having the two inequivalent ligands in a *trans* geometry from which the anionic ligand in a five-membered *P*,*N*-coordinating chelate ring (Figure 4). This means that indeed a proton of the least acidic aliphatic urea proton was transferred to the acac$^-$ ligand. Furthermore, the crystal structure shows that one CO ligand remained coordinated, revealing that **C4** is of the form [Rh(**L1**-κ^2*P*,*N*)(**L1**-κ*P*)(CO)]. In the crystal structure, two **C4** molecules are linked by intermolecular N–H···O hydrogen bonds. Although in the crystal structure there is no intramolecular hydrogen bonding between the two coordinated ligands, the DFT-optimized structure does show a intramolecular hydrogen bond between the two ligands (1.932 Å).[11] In the ^1H NMR spectrum the single aliphatic urea proton (CH_2NH) shows a strong downfield shift, which supports that the two ligands indeed interact via hydrogen bonding in solution. In addition, DFT calculations show that the optimized structure of **C4**, containing an intramolecular hydrogen bond, is 6.4 kcal mol^{-1} more stable than the optimized structure of **C4**, that does not contain an intramolecular hydrogen bond.[11]

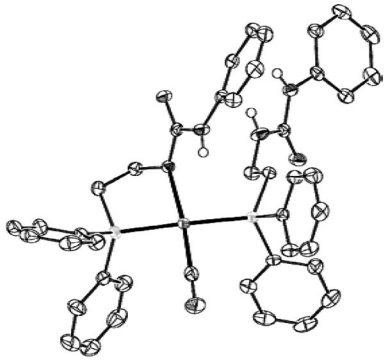

Figure 4. Displacement ellipsoid plot (50% probability level) of **C4** [Rh(**L1**-κ^2*P*,*N*)(**L1**-κ*P*)(CO)]·2(CD_2Cl_2). CH hydrogen atoms and solent molecules have been omitted for clarity.

Addition of one equivalent of **L1** to [Rh(acac)(cod)] in $CDCl_3$ resulted in a similar reaction of the ligand as in **C4**, giving a new complex (**C5**).[13] The $^{31}P\{^1H\}$ NMR spectrum showed a doublet, resonating at δ = 20.7 ppm ($^1J_{P\text{-}Rh}$ = 148 Hz). In the ^1H NMR spectrum, the evolution of *H*acac was visible. Because in the ^1H NMR spectrum also the aliphatic urea proton of the ligand has disappeared, the ureaphosphane probably coordinated as an anionic *P*,*N*-coordinating chelate as in **C4**. Mass spectrometry supports that the structure of **C5** is of the form [Rh(**L1**-κ^2*P*,*N*)(cod)]. The DFT-optimized structure of **C5** supports such a structure, showing **L1** as an anionic *P*,*N*-coordinating ligand (Figure 2).

The rich coordination chemistry of ureaphosphane **L1** was demonstrated by the preparation of complexes **C1**–**C5**. These complexes likely lead to very different behavior in catalysis. Therefore, we prepared chiral analogues of **C1**–**C5**, which were investigated in the asymmetric hydrogenation reaction. For this purpose, the chiral ureaphosphanes **L2** and **L3** were employed, which are structurally similar to **L1** (Figure 5). Ureaphosphane **L2** contains a stereogenic phosphepine backbone, an ethyl spacer and a phenylurea motif. The structure of **L3** is similar to **L2**, only **L3** contains two additional stereogenic carbon atoms in the spacer.

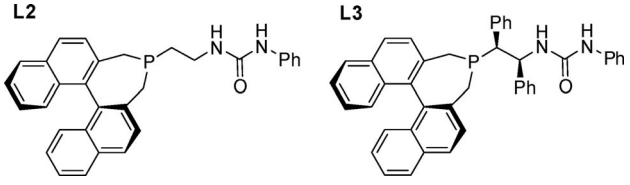

Figure 5. Structures of the chiral ureaphosphanes **L2** and **L3**.

Three different olefinic substrates were hydrogenated: methyl 2-acetamidoacrylate (**S1**), dimethyl itaconate (**S2**) and *N*-(3,4-dihydro-2-naphthalenyl)acetamide (**S3**). **S1** and **S2** are frequently used benchmark substrates in the asymmetric hydrogenation reaction, however, **S3** is a relatively difficult substrate to hydrogenate and only few systems are

reported that provide high enantioselectivity for this substrate.[18] The reaction mixtures were prepared in situ by addition of solvent (CH_2Cl_2) to a mixture of the appropriate amounts of metal precursor, ligand and substrate. Next, the reaction mixtures were put under an atmosphere of dihydrogen. The results of the asymmetric hydrogenation of **S1**, **S2** and **S3** are presented in Table 1.

Table 1. Asymmetric hydrogenation of **S1**, **S2** and **S3**.[a]

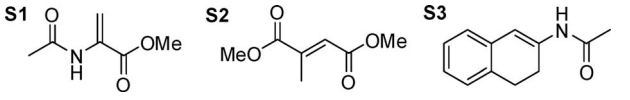

Entry	Complex	sub	Conv. (%)	*ee* (%)
1	[Rh(**L2**)$_2$(nbd)]BF_4	**S1**	100	57.4 (*S*)
2[b]	[Rh(**L2**-κ^2*P*,*O*)(nbd)]BF_4	**S1**	100	4.2 (*R*)
3	[RhCl(**L2**)(cod)]	**S1**	0	–
4	[Rh(**L2**-κ^2*P*,*N*)(**L2**-κ*P*)(CO)]	**S1**	0	–
5	[Rh(**L2**-κ^2*P*,*N*)(cod)]	**S1**	20.5	69.2 (*S*)
6	[Rh(**L2**)$_2$(nbd)]BF_4	**S2**	74.8	23.2 (*S*)
7[b]	[Rh(**L2**-κ^2*P*,*O*)(nbd)]BF_4	**S2**	100	3.8 (*R*)
8	[RhCl(**L2**)(cod)]	**S2**	6.5	4.1 (*R*)
9	[Rh(**L2**-κ^2*P*,*N*)(**L2**-κ*P*)(CO)]	**S2**	2.4	9.2 (*S*)
10	[Rh(**L2**-κ^2*P*,*N*)(cod)]	**S2**	6.8	24.3 (*R*)
11[c]	[Rh(**L2**)$_2$(nbd)]BF_4	**S3**	100	55.3 (+)
12[c]	[Rh(**L2**-κ^2*P*,*O*)(nbd)]BF_4	**S3**	100	56.5 (+)
13[c]	[RhCl(**L2**)(cod)]	**S3**	77.6	15.1 (+)
14[c]	[Rh(**L2**-κ^2*P*,*N*)(cod)]	**S3**	100	13.9 (+)
15[c]	[Rh(**L3**)$_2$(nbd)]BF_4	**S3**	26.2	85.2 (+)
16[d]	[Rh(**L3**-κ^2*P*,*O*)(nbd)]BF_4	**S3**	100	86.1 (+)
17[d]	[RhCl(**L3**)(cod)]	**S3**	71.1	26.3 (+)
18[d]	[Rh(**L3**-κ^2*P*,*N*)(**L3**-κ*P*)(CO)]	**S3**	0	–
19[d]	[Rh(**L3**-κ^2*P*,*N*)(cod)]	**S3**	100	11.2 (+)

[a] Reaction conditions: [Rh] = 1 mM, [S] = 100 mM, reaction time: 12 h, temperature: room temp., pressure: 20 bar H_2, solvent: CH_2Cl_2. [b] Formation of rhodium black. [c] [S] = 50 mM, pressure: 40 bar H_2, reaction time: 72 h. [d] [S] = 50 mM.

It appeared that for **S1** and **S2** the cationic rhodium complexes gave significantly higher conversions than the neutral rhodium complexes. For instance, **S1** was hydrogenated by the two cationic complexes (entry 1 and 2) to full conversion, while the neutral complexes gave relatively low conversions (entry 3, 4 and 5). Likely, the neutral complexes, [RhCl(**L2**)(cod)] and [Rh(**L2**-κ^2*P*,*N*)(cod)] that contain the strongly σ-donating ureaphosphane are too electron-rich, which hampers substrate coordination to the metal center.[19] On the other hand, the neutral complex [Rh(**L2**-κ^2*P*,*N*)(**L2**-κ*P*)(CO)] is coordinatively saturated, which leaves no vacant site for coordination of the substrate.[20] Nevertheless, the highest *ee* for the hydrogenation of both **S1** (69.2%, entry 5) and **S2** (24.3%, entry 10) was obtained using the neutral complex [Rh(**L2**-κ^2*P*,*N*)(cod)]. With the cationic complex [Rh(**L2**)$_2$(nbd)]BF_4 slightly lower *ee* values for **S1** (57.4%, entry 1) and **S2** (23.2%, entry 6) were obtained. The cationic complex [Rh(**L2**-κ^2*P*,*O*)(nbd)]-BF_4 seemed relatively unstable in the hydrogenation of **S1** and **S2** because after completion of the reaction rhodium black was observed in the reaction mixture. The instability of this complex possibly explains the low *ee* values obtained (entry 2 and 7).

Interestingly, the asymmetric hydrogenation of **S3**, using the neutral complexes [RhCl(**L2**)(cod)] and [Rh(**L2**-κ^2*P*,*N*)(cod)], led to relatively high conversions (entry 13 and 14). Furthermore, in the hydrogenation of **S3** using [Rh(**L2**-κ^2*P*,*O*)(nbd)]BF_4 no decomposition of the catalyst was observed in the reaction mixture after the reaction (entry 12). These results suggest that **S3** coordinates more strongly to the metal center, which explains the higher conversions obtained using [RhCl(**L2**)(cod)] and [Rh(**L2**-κ^2*P*,*N*)(cod)] and the absence of decomposition using [Rh(**L2**-κ^2*P*,*O*)(nbd)]BF_4. Although the neutral complexes [RhCl(**L2**)(cod)] and [Rh(**L2**-κ^2*P*,*N*)(cod)] provided relatively good conversion in the hydrogenation of **S3**, the obtained enantioselectivities were poor (entry 13 and 14) However, both cationic complexes [Rh(**L2**)$_2$(nbd)]BF_4 (55.3%, entry 11) and [Rh(**L2**-κ^2*P*,*O*)(nbd)]BF_4 (56.5%, entry 12) led to moderate enantioselectivities. Because relatively good conversions were obtained for substrate **S3**, this substrate was additionally investigated using the chiral ureaphosphane **L3**. With the complexes [RhCl(**L3**)(cod)] and [Rh(**L3**-κ^2*P*,*N*)(cod)] again high conversion was obtained, but the enantioselectivity was disappointing (entry 17 and 19). Interestingly, hydrogenation of **S3** using [Rh(**L3**)$_2$(nbd)]BF_4 led to an *ee* of 85.2%, although the conversion was only 26.2% (entry 15). Possibly, the additional bulky phenyl substituents in the spacer of **L3** decrease the activity of this complex because of steric reasons. However, using [Rh(**L3**-κ^2*P*,*O*)(nbd)]BF_4 an *ee* value of 86.1% obtained at full conversion (entry 16). The use of [Rh(**L3**-κ^2*P*,*N*)(**L3**-κ*P*)(CO)] could not improve these results (entry 18), which seems logical because the substrate is less likely to influence the creation of a vacant site on the metal center.

Conclusions

In summary, new ureaphosphane-rhodium(I) complexes have been synthesized, which show the rich coordination chemistry of these ligands. Depending on the nature of the anion and the ligand/metal ratio, the ureaphosphane acts either as a hybrid *P*,*O*-coordinating chelate, as an anionic *P*,*N*-coordinating chelate or as a supramolecular (hydrogen-bonded) bidentate ligand. These differences in coordination chemistry are translated into the results in catalysis, involving asymmetric ureaphosphanes. The activity and the enantioselectivity showed to be strongly dependent on the complex used. In addition, for a different substrate also a different complex was required to obtain the best activity and enantioselectivity. These results demonstrate that employing the different coordination modes of ureaphosphanes in catalysis is a valuable strategy to enlarge the substrate scope of these ligands.

Experimental Section

General Procedures: Unless stated otherwise, reactions were carried out under an inert atmosphere of nitrogen or argon using standard Schlenk techniques. CH_2Cl_2 was distilled from CaH_2; hexanes were

distilled from sodium under a nitrogen atmosphere. All reagents were purchased from commercial suppliers and were used without further purification. **L1**, **L2** and **L3** were synthesized according to a published procedure.[9] **S3** was synthesized according to a published procedure.[21] NMR spectra were measured on a Varian Mercury (^{1}H: 300 MHz, ^{31}P{^{1}H}: 121.5 MHz and ^{13}C{^{1}H}: 75.5 MHz) or a Varian Inova spectrometer (^{1}H: 500 MHz, ^{31}P{^{1}H}: 202.3 MHz, ^{13}C{^{1}H}: 125.7 MHz) at room temperature. Chemical shifts are reported in ppm and are given relative to TMS (^{1}H and ^{13}C{^{1}H}) or H_3PO_4 (^{31}P{^{1}H}) as external standards. High resolution mass spectra (HRMS) were recorded at the department of mass spectrometry at the University of Amsterdam using FAB^+ ionization on a JEOL JMS SX/SX102A four sector mass spectrometer with 3-nitrobenzyl alcohol as the matrix. IR spectra were recorded on a Thermo, Nicolet Nexus 670 FT-IR apparatus.

General Procedure Complex Synthesis: To a Schlenk flask, filled with the appropriate amounts of ureaphosphane and metal precursor, was added CH_2Cl_2. After five minutes of vigorous stirring, solvents were evaporated in vacuo.

[Rh(L1)$_2$(nbd)]BF$_4$ (C1): Yellow powder. ^{1}H NMR ($CDCl_3$, 500 MHz): δ = 1.522 (s, 2 H, Rh-nbd), 2.407 (br. s, 4 H, C*H*$_2$CH$_2$NH), 3.497 (br. s, 4 H, C*H*$_2$NH), 3.875 (s, 2 H, Rh-nbd), 4.445 (s, 4 H, Rh-nbd), 5.975 (br., 2 H, CH$_2$N*H*), 6.959 (t, J = 6.9 Hz, 2 H, ArH), 7.1–7.2 (m, 6 H, 5 ArH + 1 N*H*Ph), 7.3–7.5 (m, 24 H, ArH) ppm. ^{31}P{^{1}H} NMR ($CDCl_3$, 202.3 MHz): δ = 18.4 (d, $^1J_{P\text{-}Rh}$ = 152 Hz) ppm. ^{13}C{^{1}H} NMR ($CDCl_3$, 125.7 MHz): δ = 27.418 (CH_2), 37.005 (CH_2), 53.027 (Rh-nbd) 68.89 (Rh-nbd, CH_2), 81.898 (Rh-nbd, CH), 119.138 (CH), 122.325 (CH), 128.876 (CH), 129.48 (CH), 131.384 (CH), 132.539 (CH), 139.631 (C_{quat}), 155.835 (NH*C*ONH) ppm. HRMS (FAB^+): *m*/*z* calculated for $C_{49}H_{50}O_2N_4P_2Rh$ ([MH]$^+$): 891.2464; observed: 891.2468.

[Rh(L1-κ^2*O*,*P*)(nbd)]BF$_4$ (C2): Yellow powder. ^{1}H NMR ($CDCl_3$, 500 MHz): δ = 1.44 (s, 2 H, Rh-nbd), 2.58 (t, J = 10 Hz, 2 H, C*H*$_2$CH$_2$NH), 3.26 (s, 2 H, Rh-nbd), 3.84 (m, 2 H, C*H*$_2$NH), 3.92 (s, 2 H, Rh-nbd), 5.35 (s, 2 H, Rh-nbd), 6.68 (t, J = 5.5 Hz, 1 H, CH$_2$N*H*), 7.1–7.6 (m, 15 H, ArH), 7.71 (s, 1 H, N*H*Ph) ppm. ^{31}P{^{1}H} NMR ($CDCl_3$, 202.3 MHz): δ = 31.4 (d, $^1J_{P\text{-}Rh}$ = 170 Hz) ppm. ^{13}C{^{1}H} NMR ($CDCl_3$, 125.7 MHz): δ = 29.567 ($J_{C,P}$ = 24 Hz), 39.066 ($J_{C,P}$ = 3.2 Hz), 51.9981 (Rh-nbd), 64.116 (Rh-nbd), 90.512 (Rh-nbd), 120.729, 124.234, 128.648, 128.813, 129.010, 129.286, 129.369, 131.435, 132.657, 132.754, 137.365, 161.506 (NH*C*ONH) ppm. HRMS (FAB^+): *m*/*z* calculated for $C_{28}H_{29}N_2OPRh$ ([MH]$^+$): 543.1073; observed: 543.1074. Solution IR (20 mM, $CDCl_3$), $\tilde{\nu}$ = 1572 cm^{-1} (CO_{urea} band).

[RhCl(L1)(cod)] (C3): Yellow powder. ^{1}H NMR ($CDCl_3$, 500 MHz): δ = 1.88 (s, 2 H, Rh-cod), 2.03 (s, 2 H, Rh-cod), 2.33 (d, J = 6 Hz, 4 H, Rh-cod), 2.76 (m, 2 H, C*H*$_2$CH$_2$NH), 3.09 (s, 2 H, Rh-cod), 3.98 (q, J = 6.5 Hz, 2 H, C*H*$_2$NH), 5.48 (s, 2 H, Rh-cod), 6.35 (s, 1 H, N*H*CH$_2$), 6.79 (s, 1 H, N*H*Ph), 7.02 (t, J = 7 Hz, 1 H, ArH), 7.2–7.7 (m, 14 H, ArH) ppm. ^{31}P{^{1}H} NMR ($CDCl_3$, 202.3 MHz): δ = 21.1 (d, $^1J_{P\text{-}Rh}$ = 148 Hz) ppm. ^{13}C{^{1}H} NMR ($CDCl_3$, 125.7 MHz): δ = 28.897, 29.103, 33.053, 37.573, 71.465, 105.471, 119.526, 122.796, 128.478, 128.551, 129.093, 130.411, 132.322, 132.653, 133.484, 133.567, 139.322, 155.631 (NH*C*ONH) ppm. HRMS (FAB^+): *m*/*z* calculated for $C_{29}H_{34}ClN_2OPRh$ ([MH]$^+$): 595.1152; observed: 595.1164.

[Rh(L1-κ^2*P*,*N*)(L1)(CO)] (C4): Yellow-orange powder. ^{1}H NMR ($CDCl_3$, 500 MHz): δ = 2.35 (t, J = 7 Hz, 2 H, CH_2), 2.65 (br. s, 2 H, CH_2), 3.43 (br. s, 2 H, CH_2), 3.8 (br. s, 2 H, CH_2), 6.44 (s, 1 H, ArH), 6.7 (br. s, 1 H, N*H*CH$_2$), 6.75–7.75 (m, 30 H, 29 ArH + 1 NHPh), 8.0 (s, 1 H, NHPh) ppm. ^{31}P{^{1}H} NMR ($CDCl_3$, 202.3 MHz): δ = 19.7 (dd, $^1J_{P\text{-}Rh}$ = 136, $^2J_{P,P}$ = 310 Hz), 52.2 (dd, $^1J_{P\text{-}Rh}$ = 129, $^2J_{P,P}$ = 310 Hz) ppm. ^{13}C{^{1}H} NMR ($CDCl_3$, 125.7 MHz): δ = 29.303 (d, $J_{C,P}$ = 22 Hz, CH_2), 31.006 (d, $J_{C,P}$ = 33 Hz, CH_2), 35.849 (d, $J_{C,P}$ = 8.7 Hz, CH_2), 47.283 (d, $J_{C,P}$ = 5.9 Hz, CH_2), 118.298, 118.592, 121.067, 121.269, 128.499, 128.549, 128.852, 128.926, 129.041, 129.059, 130.478, 130.832, 132.793, 132.889, 133.073, 133.170, 133.413, 133.757, 134.368, 134.699, 140.417, 140.477, 155.785 (NH*C*ONH) 162.215 (N*C*ONH), 192 (br., Rh-*C*O) ppm. HRMS (FAB^+): *m*/*z* calculated for $C_{43}H_{42}O_3N_4P_2Rh$ ([MH]$^+$): 827.1787; observed: 827.1784. Solution IR (20 mM, $CDCl_3$), $\tilde{\nu}$ = 1981 cm^{-1} (Rh–CO band).

[Rh(L1-κ^2*P*,*N*)(cod)] (C5): Yellow powder. ^{1}H NMR ($CDCl_3$, 500 MHz): δ = 2.77 (m, 2 H, C*H*$_2$CH$_2$N), 3.96 (m, 2 H, C*H*$_2$N), 7.0–7.7 (m, 16 H, 15 ArH + 1 N*H*Ph) ppm. ^{31}P{^{1}H} NMR ($CDCl_3$, 202.3 MHz): δ = 20.7 (d, $^1J_{P\text{-}Rh}$ = 148 Hz) ppm. HRMS (FAB^+): *m*/*z* calculated for $C_{29}H_{33}N_2OPRh$ ([MH]$^+$): 559.1386; observed: 559.1373. The presence of side product in the catalyst mixture prevented to report unambiguously the ^{13}C{^{1}H} NMR signals.

General Procedure Hydrogenation Experiments: The hydrogenation experiments were carried out in an Accelerator SLT workstation of Chemspeed Technologies (Http://www.chemspeed.com) under inert conditions. The reaction mixtures were prepared in situ by addition of CH_2Cl_2 to a Schlenk flask filled with the appropriate amounts of metal precursor, ligand and substrate. The reaction mixtures were subsequently injected manually into a reaction vial of the Accelerator SLT workstation. Next, the automated program of the Accelerator SLT workstation was started, putting the reaction mixtures under an atmosphere of dihydrogen and mixing the reaction mixtures by vortex shaking. Product samples of methyl-2-acetamidoacrylate (**S1**), dimethyl itaconate (**S2**) and *N*-(3,4-dihydro-2-naphthalenyl)acetamide (**S3**) were prepared directly after completion of the program and analyzed by using an Interscience Trace GC Ultra (FID detector) for **S1** and **S3** or an Interscience Focus GC for **S2**. Both GC's were equipped with a CP-Chiralsil-DexCB column. For **S3** the signs were reported to emphasize changes in the absolute chirality of the product as measured by GC, however, they do not reflect a measured optical rotation.

X-ray Crystallography of C4: $C_{43}H_{41}N_4O_3P_2Rh{\cdot}2(CD_2Cl_2)$, a = 11.8876(3), b = 12.0474(3), c = 16.8658(5) Å, α = 75.752(2), β = 89.596(2), γ = 75.529(2)°, triclinic, $P\bar{1}$, Z = 2, Mw = 1000.51, Dx = 1.469 g/cm^3. Mo-K_α, λ = 0.71073 Å, T = 150 K. X-ray data were collected on a Nonius KappaCCD [10391 unique reflections, θ(max) = 27.5°]. The images were processed with EVALCCD. The structure was solved with DIRDIF99 and refined with SHELXL-97. One of the two CD_2Cl_2 solvent molecules was refined with a disorder model (0.621:0.379). R = 0.0282 [8944 reflections with $I > 2\sigma(I)$], $wR2$ = 0.0699 (10393 reflections), S = 1.058, 569 refined parameters, residual density range –0.63:0.44 e/Å^3. The structure was validated with PLATON/CheckCIF.

CCDC-743287 (for **C4**) contains the supplementary crystallographic data for this paper. These data can be obtained free of charge from The Cambridge Crystallographic Data Centre via www.ccdc.cam.ac.uk/data_request/cif.

Dilution Studies: ^{1}H NMR dilution experiments were carried out by preparing a 0.5 mL sample at a known concentration: 10, 20, 30 and 40 mM in $CDCl_3$ for **L1** and for **C3**. The position of the solvent signal was used as a reference for the urea NH signal.

DFT Calculations: The geometry optimizations were carried out with the Turbomole program[22] coupled to the PQS Baker optimizer.[23] Geometries were fully optimized at the BP86[24] level using the SV(P) basis set[25] on all atoms (small-core pseudopotential[26] on rhodium).

Supporting Information (see also the footnote on the first page of this article): Optimized geometries of the species of the DFT calculations are supplied as pdb files.

Acknowledgments

This research is financially supported by BASF B.V., The University of Amsterdam and The Netherlands and the Dutch Ministry of Economic Affairs by way of SenterNovem. J. W. H. Peeters is acknowledged for the mass spectrometric experiments. The Nederlandse Organisatie voor Wetenschappelijk Onderzoek, Chemische Wetenschappen (NWO-CW) is kindly acknowledged for financial support to A. L. S.

[1] For reviews see: a) M. J. Wilkinson, P. W. N. M. van Leeuwen, J. N. H. Reek, *Org. Biomol. Chem.* **2005**, *3*, 2371–2383; b) B. Breit, *Angew. Chem. Int. Ed.* **2005**, *44*, 6816–6825; c) A. J. Sandee, J. N. H. Reek, *Dalton Trans.* **2006**, 3385–3391.

[2] a) F. W. Patureau, M. Kuil, A. J. Sandee, J. N. H. Reek, *Angew. Chem. Int. Ed.* **2008**, *47*, 3180–3183; b) B. Breit, W. Seiche, *J. Am. Chem. Soc.* **2003**, *125*, 6608–6609; c) B. Breit, W. Seiche, *Angew. Chem. Int. Ed.* **2005**, *44*, 1640–1643; d) M. Weis, C. Waloch, W. Seiche, B. Breit, *J. Am. Chem. Soc.* **2006**, *128*, 4188–4189; e) F. Chevallier, B. Breit, *Angew. Chem. Int. Ed.* **2006**, *45*, 1599–1602; f) C. Waloch, J. Wieland, M. Keller, B. Breit, *Angew. Chem. Int. Ed.* **2007**, *46*, 3037–3039; g) M. de Greef, B. Breit, *Angew. Chem. Int. Ed.* **2009**, *48*, 551–554; h) Y. Liu, C. A. Sandoval, Y. Yamaguchi, X. Zhang, Z. Wang, K. Kato, K. Ding, *J. Am. Chem. Soc.* **2006**, *128*, 14212–14213.

[3] a) V. F. Slagt, M. Röder, P. C. J. Kamer, P. W. N. M. van Leeuwen, J. N. H. Reek, *J. Am. Chem. Soc.* **2004**, *126*, 4056–4057; b) X.-B. Jiang, L. Lefort, A. H. M. de Vries, P. W. N. M. van Leeuwen, J. G. de Vries, J. N. H. Reek, *Angew. Chem. Int. Ed.* **2006**, *45*, 1223–1227; c) M. Kuil, P. E. Goudriaan, P. W. N. M. van Leeuwen, J. N. H. Reek, *Chem. Commun.* **2006**, 4679–4681; d) M. Kuil, P. E. Goudriaan, A. W. Kleij, D. M. Tooke, A. L. Spek, P. W. N. M. van Leeuwen, J. N. H. Reek, *Dalton Trans.* **2007**, 2311–2320; e) J. M. Takacs, D. S. Reddy, S. A. Moteki, D. Wu, H. Palencia, *J. Am. Chem. Soc.* **2004**, *126*, 4494–4495; f) J. M. Takacs, K. Chaiseeda, S. A. Moteki, D. S. Reddy, D. Wu, K. Chandra, *Pure Appl. Chem.* **2006**, *78*, 501–509; g) S. A. Moteki, J. M. Takacs, *Angew. Chem. Int. Ed.* **2008**, *47*, 894–897.

[4] a) H. Gulyás, J. Benet-Buchholz, E. C. Escudero-Adan, Z. Freixa, P. W. N. M. van Leeuwen, *Chem. Eur. J.* **2007**, *13*, 3424–3430; b) L. Pignataro, B. Lynikaite, J. Cvengroš, M. Marchini, U. Piarulli, C. Gennari, *Eur. J. Org. Chem.* **2009**, 2539–2547; c) Y. Li, Y. Feng, Y.-M. He, F. Chen, J. Pan, Q.-H. Fan, *Tetrahedron Lett.* **2008**, *49*, 2878–2881.

[5] L. K. Knight, Z. Freixa, P. W. N. M. van Leeuwen, J. N. H. Reek, *Organometallics* **2006**, *25*, 954–960.

[6] A. J. Sandee, A. M. van der Burg, J. N. H. Reek, *Chem. Commun.* **2007**, 864–866.

[7] J. Meeuwissen, M. Kuil, A. M. van der Burg, A. J. Sandee, J. N. H. Reek, *Chem. Eur. J.* **2009**, *15*, 10272–10279.

[8] P. A. Duckmanton, A. J. Blake, J. B. Love, *Inorg. Chem.* **2005**, *44*, 7708–7710.

[9] J. Meeuwissen, R. J. Detz, A. J. Sandee, B. de Bruin, J. N. H. Reek, *Dalton Trans.* **2010**, *39*, 1929–1931.

[10] For an account on intra- and intermolecular interactions, see: A. Mulder, J. Huskens, D. N. Reinhoudt, *Org. Biomol. Chem.* **2004**, *2*, 3409–3424.

[11] See Supporting Information.

[12] a) L. Song, P. Stang, *Inorg. Chim. Acta* **1991**, *188*, 107–111; b) M. Kuriyama, K. Nagai, K.-i. Yamada, Y. Miwa, T. Taga, K. Tomioka, *J. Am. Chem. Soc.* **2002**, *124*, 8932–8939.

[13] For reviews on hemilabile ligands, see: a) P. Braunstein, F. Naud, *Angew. Chem. Int. Ed.* **2001**, *40*, 680–699; b) P. Braunstein, *J. Organomet. Chem.* **2004**, *689*, 3953–3967; c) A. Bader, E. Lindner, *Coord. Chem. Rev.* **1991**, *108*, 27–110.

[14] Addition of more equivalents of **L1** led to a mixture of species.

[15] For a related system, see: C. Meyer, M. Scherer, H. Schönberg, H. Rüegger, S. Loss, V. Gramlich, H. Grützmacher, *Dalton Trans.* **2006**, 137–148.

[16] Using only one equivalent of **L1** also led to the evolution of *H*acac. The $^{31}P\{^{1}H\}$ NMR spectrum showed a doublet, resonating at δ = 39.8 ppm ($^{1}J_{P\text{-}Rh}$ = 171 Hz), that likely belongs to [Rh(**L1**-κ^2*P*,*N*)$(CO)_x$]. However, we were unable to fully characterize this species.

[17] For a related system, see: J. A. Fuentes, M. L. Clarke, A. M. Z. Slawin, *New J. Chem.* **2008**, *32*, 689–693.

[18] F. W. Patureau, S. de Boer, M. Kuil, J. Meeuwissen, P.-A. R. Breuil, M. A. Siegler, A. L. Spek, A. J. Sandee, B. de Bruin, J. N. H. Reek, *J. Am. Chem. Soc.* **2009**, *131*, 6683–6685 (*ee* 81%) and reference 3b (*ee* 94%).

[19] Likely, the neutral complexes [RhCl(**L2**)(cod)] and [Rh(**L2**-κ^2*P*,*N*)(cod)] lose the cod ligand and remain inactive in the reaction mixture as Rh^{III} dihydride species, due the low affinity of these complexes towards substrates **S1** and **S2**.

[20] For an example involving $Rh(acac)(CO)_2$ as a precursor for an active hydrogenation catalyst, see: C. J. Scheuermann née Taylor, C. Jaekel, *Adv. Synth. Catal.* **2008**, *350*, 2708–2714.

[21] J. L. Renaud, P. Dupau, A.-E. Hay, M. Guingouain, P. H. Dixneuf, C. Bruneau, *Adv. Synth. Catal.* **2003**, *345*, 230–238.

[22] a) R. Ahlrichs, M. Bär, H.-P. Baron, R. Bauernschmitt, S. Böcker, M. Ehrig, K. Eichkorn, S. Elliott, F. Furche, F. Haase, M. Häser, C. Hättig, H. Horn, C. Huber, U. Huniar, M. Kattannek, A. Köhn, C. Kölmel, M. Kollwitz, K. May, C. Ochsenfeld, H. Öhm, A. Schäfer, U. Schneider, O. Treutler, K. Tsereteli, B. Unterreiner, M. von Arnim, F. Weigend, P. Weis, H. Weiss, *Turbomole*, version 5, January **2002**. Theoretical Chemistry Group, University of Karlsruhe; b) O. Treutler, R. Ahlrichs, *J. Chem. Phys.* **1995**, *102*, 346–354.

[23] a) PQS version 2.4, **2001**, Parallel Quantum Solutions, Fayetteville, Arkansas, USA (the Baker optimizer is available separately from PQS upon request); b) J. Baker, *J. Comput. Chem.* **1986**, *7*, 385–395.

[24] a) A. D. Becke, *Phys. Rev. A* **1988**, *38*, 3098–3100; b) J. P. Perdew, *Phys. Rev. B* **1986**, *33*, 8822–8824.

[25] A. Schäfer, H. Horn, R. Ahlrichs, *J. Chem. Phys.* **1992**, *97*, 2571–2577.

[26] a) Turbomole basisset library, *Turbomole Version 5*; b) D. Andrae, U. Haeussermann, M. Dolg, H. Stoll, H. Preuss, *Theor. Chim. Acta* **1990**, *77*, 123–141.

Received: February 22, 2010
Published Online: May 14, 2010

